Research Square

Preprints are preliminary reports that have not undergone peer review.
They should not be considered conclusive, used to inform clinical practice,
or referenced by the media as validated information.

Antibacterial Mechanism of N-PMI and the Characteristics of PMMA-co-N-PMI Copolymer

Han Shi
East China University of Science and Technology
Qixin Zhuang
East China University of Science and Technology
Anna Zheng
East China University of Science and Technology
Pengfei Zhan
East China University of Science and Technology
Yong Guan (yguan@ecust.edu.cn)
East China University of Science and Technology https://orcid.org/0000-0002-9861-4785
Dafu Wei
East China University of Science and Technology
Xiang Xu
East China University of Science and Technology
Tao Wu
East China University of Science and Technology

Research Article

Keywords: N-PMI, Antimicrobial activity, Fluorescence quenching experiment, Antimicrobial mechanism, azeotropic copolymerization.

Posted Date: September 8th, 2021

DOI: https://doi.org/10.21203/rs.3.rs-872816/v1

License: This work is licensed under a Creative Commons Attribution 4.0 International License.
Read Full License

Abstract

Aiming at the excellent killing effect of N-phenylmaleimide (N-PMI) on microorganisms, this paper used structural simulation analysis, fluorescence analysis, confocal laser scanning microscope and SEM to find that the double bond in N-PMI could interact with the sulfur groups in the membrane protein, changing its conformation, rupturing the plasma membrane of the cell, leaking the contents, and ultimately causing the death of the microorganisms. Therefore, once the double bond participated in the polymerization, N-PMI loosed its antimicrobial function. N-PMI could achieve azeotropic copolymerization with MMA through reactive extrusion polymerization, and didn't follow the law of reactivity ratio of classic copolymerization. N-PMI with a content of 5% can be evenly inserted into the PMMA chain segment during the copolymerization reaction, thereby increasing the Tg of pure PMMA by up to 15°C, which provided the PMMA-co-PMI copolymer with resistance to boiling water sterilization advantageous conditions. In addition, the copolymer was superior to the commercially available pure PMMA in terms of bending strength and modulus. At the same time, N-PMI with a content of 5% has little effect on the transparency of PMMA after participating in the copolymerization. Moreover, the trace amount of residual N-PMI made the material have excellent antimicrobial function, and the bacteriostatic zone is extremely small, which provided an excellent guarantee for the safety and durability of the material. As a medical biological material, the PMMA-co-PMI copolymer has a good industrialization application prospects.

1 Introduction

There are a large number of microorganisms in our environment, but some harmful microorganisms (especially bacteria and fungi) directly threaten human safety and health[1–4]. Infectious diseases caused by bacteria and fungi, such as plague, diphtheria, tuberculosis, etc. appear frequently in clinic practice and bring great harm to human society[1, 5]. In addition, bacteria will produce biofilms and adhere to the surface of various materials, thereby affecting the physicochemical properties and functions of materials, such as the adhesion and erosion of marine microorganisms to the surface of the hull. Therefore, various antibacterial agents and antibacterial materials are receiving extensive attention, and how to use antibacterial agents to effectively inhibit the growth and reproduction of harmful microorganisms has also become a crucial issue[6, 7].

N-phenylmaleimide (N-PMI) is a modification monomer with five-member imide ring that restricts the movement of polymer chains, which can improve the thermal stability, impact resistance and processing properties of the material[8–10]. Therefore, N-PMI can be used as heat-resistant modifier, vulcanization crosslinking agent, pharmaceutical intermediate, antifouling agent, and antibacterial agent in various occasions[11, 9]. At the beginning, N-PMI attracted people's attention as antifouling agent. It could effectively prevent the attachment and reproduction of marine organisms without polluting water, nor corroding equipment and metals. Importantly, N-PMI has extensive antibacterial activity against microorganisms such as Escherichia coli (E. coli), Staphylococcus aureus (S. aureus), Candida albicans etc., and can effectively inhibit the growth and reproduction of microorganisms[12–18]. In addition, N-

PMI and its derivatives have a certain anti-tumor activity[19–21] and anti-inflammatory activity[22]. In the context of the continued epidemic of COVID-19, N-PMI must have a wide range of applications in the biological and medical fields.

However, the exploration of the antibacterial mechanism of N-PMI is still in its infancy, and its antibacterial mechanism is still unclear. Cechinel-Filho[23] mentioned that the antibacterial activity of N-PMI resulted from its hydrophobicity (logP = 1.35) and electrically neutral, which enable it to pass through the cell membrane and cause the death of bacteria. Sortino[15] researched the N-phenyl maleimide and the N-phenylalkyl maleimides with different carbon numbers and it was found that the antibacterial activity of N-PMI was closely related to the five-membered imide ring. In addition, as the carbon number of the N-phenylalkyl group increased, the antibacterial performance of the corresponding maleimides did not decrease significantly. Yunes[21] found that the antibacterial properties of N-PMI with different benzene substituents were different. This was because the electronegativity of the substituents would affect the interaction between maleimides and bacteria. The research results of Natalia S. et al.[24] showed that N-substituted maleimides affected biosynthesis of chitin and β (1,3) glucan, components of the fungal cell wall.

Furthermore, Karina[25] believed that N-PMI could trigger the apoptosis of erythrocyte, tumor cells, etc. and showed obviously the characteristic behaviors of apoptosis via flow cytometry, fluorescene microscopy and Annexin V-FITC assay. Apoptosis was a kind of autonomous and programmed cell death progress (PCD), generally started from the combination of receptors on the plasma membrane and related apoptosis factors. Next, the processes including the interaction between apoptosis regulatory molecules and the activation of proteolytic enzymes were conducted, eventually leading to cell apoptosis. Therefore, it was speculated that the bacteria membrane protein was the putative primary target of N-PMI, then the membrane protein conformation was changed, which finally led to the damage of cell membrane and the death of the bacteria[26].

In terms of molecular structure, the C = C bond of N-PMI with high electron-deficient property and high chemical reactivity was easy to undergo nucleophilic addition reaction, Diels-Alder addition reaction, Michael reaction, anionic and free radical polymerization reaction[27–29]. Nair et al.[30] reported the Michael addition reaction of N-PMI and thiophenol. No catalysts and additives were needed, after the reaction between them for 15 minutes at room temperature using water as a solvent, the thiosuccinimides were obtained in high yield. Natalia[24] also used sulfhydryl-containing N-acetyl methyl cysteinate to simulate the reaction between maleimides and cysteinyl residues presenting at the enzyme active centers. As critical component of cell membrane, membrane protein was rich in sulfhydryl groups in reactive cysteinyl residues, also being easy to react with N-PMI, which, therefore, would further change the membrane protein conformation and lead to the change of cell membrane morphology.

In other hand, polymethyl methacrylate (PMMA) has a very wide range of applications, especially as human bones, and the transparent pool wall of marine aquariums. There is a great need for safe, long-lasting antibacterial PMMA. Therefore, based on the previous research of our laboratory on the synthesis

of PMMA and its copolymers through reactive extrusion polymerization, the copolymerization of N-PMI and MMA was implemented[31–33].

Acrylic coating has been extensively applied in building, electronic appliance, and other fields, due to its excellent properties such as aging resistance, transparency, and better decoration[34]. Especially, antimicrobial acrylic coating has broad application prospects in medical equipment, daily necessities, etc. Therefore, N-PMI could also be chosen as antibacterial agent in acrylic coating due to good solubility of organic solvents. Through the analysis of antibacterial activity under different conditions, the antibacterial mechanism of N-PMI may be further inferred, and its application direction in the field of polymer materials will be determined.

2 Materials And Methods

2.1 Materials

Methyl methacrylate (MMA), analytical grade, was provided by China's Oil Sunup Group Co., LTD(China) and obtained after reduced pressure distillation. Butyl acrylate (BA), Glycidyl methacrylate (GMA), N-phenyl maleimide (N-PMI), analytical grade, was provided by Shanghai Titan Co. Ltd. (Shanghai, China). AIBN, analytical grade, was provided by Shanghai Ling Feng Chemical Reagent Co. Ltd. (Shanghai, China), and obtained after recrystallization in hot ethanol. Homo-polymethylmethacrylate (Commercial PMMA, VH001, Mn = 4.26×10^4, MWD = 1.61) was purchased from Mitsubishi Rayon Polymer Co., Ltd(Nantong, China). All reagents were used as received.

2.2 Molecular structure and Electrostatic Potential Analysis

The optimized geometries of N-phenylmaleimide (N-PMI), N-phenylsuccinimide (N-PSI), and N-chlorophenylmaleimide (N-ChPMI) were obtained by Gaussian 09 software at the B3LYP/6-31G(d) level. On this basis, the electrostatic potential (ESP) at the VDW surface defined by Bader (i.e. an electron isodensity surface of 0.001 e $bohr^{-3}$) was calculated using Multiwfn software.

2.3 Antibacterial Activity Assay and The antibacterial rate-contact time curves

The minimum inhibitory concentration (MIC) of N-PMI, N-PSI and N-ChPMI against *E. coli* and *S. aureus* were determined by using the standardized microbroth dilution method. All samples were dissolved in 10mM phosphate buffer solution (PBS, pH 7.4) with final pH 7.4 to prepare the reserved solutions. The corresponding reserved solution was diluted to obtain a 2-fold serial dilution (2-2048mg L^{-1}) with 10mM PBS. 2mL of different diluted solutions, 2 mL of LB broth and 0.2 mL of *E. coli* and *S. aureus* with a concentration of 10^7CFU/mL were added respectively. And the suspensions were incubated at 37°C for 24 h. The antibacterial agent concentration of the highest dilution tube without bacterial growth was MIC.

The antibacterial rate-contact time curves for N-PMI were carried out against *E. coli* and *S. aureus*. The 10^8 CFU/ml bacteria suspensions mixed with 40 mg/L N-PMI, were incubated together for 10, 30, 60, 90, 120, and 240 minutes at 25°C. Then 1 mL of culture solution at different times was extracted and diluted to various dilutions (10^4 ,10^3 and 10^2 CFU/ml), respectively. Next, 0.1 ml of these cultures was seeded on agar in a petri dish, and the dishes were incubated for 24 h at 37°C. Controls were carried out in the presence of 10 mM PBS but without N-PMI. The number of colony-forming units of the surviving bacteria was counted, and the inhibition efficiency of cell growth was estimated. All assays were repeated three times.

2.4 Effect of N-PMI on fluorescence spectra of bacteria membrane protein

0.5mL bacteria suspension was added into 1.5mL of different concentrations of potassium iodide (KI), N-PSI or N-PMI in physiological saline solution and incubated for 1 h at 25°C. The emission spectra of these samples were scanned from 250 to 500 nm with a fixed excitation wavelength of 258 and 296 nm (for KI solution), only 258nm (for N-PSI and N-PMI solution). Both of the slit widths of excitation and emission spectrum were 10 nm on a LS-55 lumine/fluorescence spectrophotometer[35, 36]. In this experiment, the optimum concentration of *S. aureus* and *E. coli* was adjusted to a concentration of 2×10^8 CFU/mL in physiological saline, based on the emission fluorescence intensity.

2.5 Assays of membrane permeation and laser scanning confocal microscope (CLSM)

FITC fluorescence staining was used to visualize the leakage of cytoplasmic membrane through CLSM, as described previously. The green fluorescent probe FITC was dissolved in DMSO as the stock solution (10 mg ml^{-1}). The cell suspensions of 2×10^8 CFU/ml, were incubated with N-PMI for 60 min at 30°C. The treated cells were centrifuged, washed three times and re-suspended in the same volume of PBS. PBS control was done without N-PMI and incubated for 60min at 30°C, washed three times and re-suspended in PBS as well. FITC stock solutions of 2ml were added to experiments and controls respectively, and the solution with the final FITC concentration of 6mg/L was then incubated for 30min at 30°C. The solution was dropped to the slides then examined by CLSM, which using a laser scanning confocal microscope (AIR, Nikon, Japan) with a 405 nm semiconductor laser (Coherent) as the excitation source. The laser beam was focused by a ×60 objective to a spot of about 1 μm in diameter. The excitation power intensity used was about 250 W cm^{-2}.

2.6 Scanning electron microscope analysis (SEM)

10ml of bacterial cell suspensions, 2×10^8 CFU/mL, was centrifuged at 5050r/min for 7 min at 4℃, and discarded the supernatant. The bacteria was washed twice with PBS buffers of 10 mL centrifuged, discarded the supernatant, and used as the reference test group. 10 mL of *E. coli* and *S. aureus* bacteria suspensions were centrifuged at 8000 r/min for 5 min at 4 ℃, discarded the supernatant, and 10 mL of 40 mg/L N-PMI solution was added to the centrifuge tube. After being mixed for 2 h, 10 mL of 0.0141

mol/L sodium thiosulfate standard solution was added into it, mixed for 10 min, and centrifuged for 7 min at 4000 r/min at 4°C. After being washed twice with PBS, the bacteria suspensions were centrifuged into a pellet, discarded the supernatant, as the antibacterial test group. Then glutaraldehyde fixatives of 1 mL were added to the test groups, respectively, and stood at 4°C for 12 h.

After the fixation was completed, discarded the supernatant and rinsed with PBS 3 times. Gradient elution was performed with 20%, 50%, 80%, and 100% ethanol, respectively. After eluting for 10 minutes each time, the bacteria suspension was centrifuged at 5050r/min for 5 min. Next, the above-mentioned 100% ethanol was replaced with tert-butanol and centrifuged twice, and 2 mL tert-butanol was added and stood for 30 min at 4°C. The treated bacteria suspension was dropped to the clean silicon wafer (treated previously by UV-O_3), taking care not drip thick bacteria droplet. The silicon wafers were dried at 30°C and the microscopic morphology of the bacteria were observed by S-4800 field emission scanning electron microscope (FESEM, Hitachi, Japan), and the accelerating voltage was 10 kV.

2.7 The Leakage of K^+, Ca^{2+} and Mg^{2+} Assay

The cultured 2×10^8 CFU/mL *E. coli* and *S. aureus* suspension was centrifuged at 4000 r/min for 7 min, the supernatant was discarded, and washed with sterile saline for 3 times. In addition, the 40 mg/L N-PMI solution was prepared with sterile normal saline and 5 mL of the washed bacteria suspension was mixed with N-PMI solution. The samples of 5 mL were taken after treating for 1min, 30 min, 60 min, and 90 min, respectively, and the neutralizers (0.1 mol/L sodium thiosulfate solution) of 10 ml were added and treated for 10 min. A 0.22μm filter membrane was used to filter the bacteria suspensions. NexION 2000-(A-10) inductively coupled plasma-optical emission spectroscopy (ICP-OES) was used to determine the K^+, Ca^{2+} and Mg^{2+} concentration of filtrates[37].

2.8 Preparation of MMA-co-PMI and Acrylic Coatings

According to previous studies, N-PMI and MMA was copolymerized in a two-stage extruders. The first stage was TDE-40 co-rotating tightly meshing twin-screw extruder (D = 41.3mm, L/D = 68), and the second stage was TDY-40 counter-rotating twin-screw extruder (D = 41mm, L/D = 60). The monomers and initiators (AIBN, 0.4wt%) were mixed in tank and sent to the first barrel of the first stage extruder through a metering pump which could be accurately quantified. Before polymerization, the extruders were heated to 220°C and purged with dry argon to remove impurities. Then when the temperature dropped to the set temperature, while being fed the monomer, the extruder began to run and gradually increased the polymerization amount to the normal value. A devolatilizer was installed on 10th barrel of the second stage extruder near to the die to remove residual monomers. After the extruded polymer is stabilized, pelletizing was performed to obtain the MMA-co-PMI copolymers.

Regarding the acrylic coatings, 35 mL MMA, 10 mL BA, 5 mL GMA, and 0.25 g AIBN were mixed in a beaker, and 50 mL ethyl acetate was added to a four-necked flask. After the temperature rose to 75℃, 1/3 of mixed monomer was added to the four-necked flask, and the rest mixed monomer containing the initiator was added dropwise to the flask through a constant pressure funnel within 2 h. Under the

protection of nitrogen, the polymerization performed at 75℃ for 4 h. Finally 0.5wt% or 1wt% N-PMI was added. Until it was evenly distributed, the temperature was lowered to obtain the product. Then the product was coated into a film, and dried in stage in an oven to obtain the film samples.

2.9 Characterization of MMA-co-PMI

The molecular weight and distribution were characterized by Waters515 spectrometer connected with Wyatt Technology DAW NEOS small-angle light scattering detector. THF was used as the solvent with a sample content of 5mgml^{-1} and the test was carried out at 25°C.

The Tg of samples were measured by Diamond DSC (Perkins-Elmer, America). The samples were scanned at temperatures ranging from 25°C to 180°C in air atmosphere and the temperature was increased at the rate of 5 K min^{-1}.

The samples were molded by injection machine according to the standards GB/T 11997–2008 (China) and GB/T 15597.2–2010(China). The tensile and flexural strengths were measured through a CMT4204 microcomputer control electronic universal material testing machine at the speed of 5mm/min and 2mm/min, respectively. The impact strengths were measured by CEAST 9050 cantilever beam impact tester.

2.10 Antibacterial Test of MMA-co-PMI and Acrylic Coatings

The antimicrobial activity of the samples was analyzed by the shaking flask method. Steps: 0.10 g copolymers or coating films (before water washing, after water washing and purified) was mixed with 10 ml bacterial culture (10^5 CFU/ml), shook in a 37°C incubator for 24 h. Then they were prepared into various diluents (10^4 ,10^3 and 10^2CFU/ml) in sequence. 0.1 ml of these diluents was taken, and inoculated on the agar in a petri dish, incubated at 37°C for 24 h. The number of colonies was counted to estimate the inhibition efficiency of cell growth. Each sample was measured three times, and the average value was calculated.

The ring diffusion test was used to characterize the leaching characteristic of antibacterial materials. The sheets of MMA-co-PMI copolymers were prepared in a compression press (Guangdong Bolon Precision Testing Machines, China) at 190 ºC, 10 MPa for 5 min. The prepared samples were cut into the wafers, 20mm in diameter. The acrylic coating films also were cut into the wafers, 20mm in diameter. Then, 0.1 mL suspensions of *E. coli* and *S. aureus* with a concentration of 10^6 CFU/ml were inoculated on the agar plate in the petri dishes. The wafers above were placed on the agar plates, which were then incubated at 37°C for 24 h in an incubator before measuring the diameters of inhibition annulus. All the tests were carried out in duplicate.

3 Results And Discussion

3.1 Antibacterial Activity of N-PMI

The minimum inhibitory concentrations (MIC) of N-PMI, N-PSI and N-ChPMI against *E. coli* and *S. aureus* were shown in Table 1. It can be seen that the MICs of N-PMI against *E. coli* and *S. aureus* are 64 and 32 mg/L, respectively, and have good broad-spectrum antibacterial properties. The hydrogen atom on the benzene ring was replaced with a halogen atom to become N-ChPMI. As a result, its antibacterial activity is significantly reduced. In addition, when the double bond in N-PMI was opened by sulfur bonds, its structure is similar to N-PSI, but the antibacterial activity of N-PSI is much lower than that of N-PMI. This shows that the antibacterial activity of N-PMI is not only related to the five-membered imine ring mentioned in the previous article, but also has a very important relationship with the C = C double bond in the imine ring.

Table 1. Minimum inhibitory concentration against *E. coli* and *S. aureus* of samples

	N-PMI	N-PSI	N-ChPMI
E. coli	64	1024	256
S. aureus	32	1024	128

The antibacterial rate-contact time curves were shown in Fig. 1. When the contact time reached 120min and 360min, the antibacterial rate reached 50% and 99% respectively. It can be seen that the antibacterial effect of N-PMI is both dose-dependent and time-dependent.

3.2 Molecular Structure Simulation and Electrostatic Potential

First, the molecular structure of N-PMI, N-PSI and N-ChPMI was optimized by Gauss 09 using the B3LYP/6-31G theory, and the lowest energy and most stable molecular structure was obtained. On this basis, the Multiwfn software was used to calculate the surface electrostatic potential (ESP), and the calculation results were shown in Fig. 2. It can be seen that although N-PMI is electrically neutral as a whole, the C = C double bond region in the five-membered imine ring exhibits significant electrical positivity (+ 25kJ/mol), which makes it easier to attract the electronegative phospholipid area of the cell membrane lays the foundation for its antibacterial properties. Compared with N-PMI, the electrical positivity of N-PSI is reduced, but the difference is not very big. However, perhaps due to the lack of double bonds that can further interact with bacterial proteins through sulfur bonds, its antibacterial properties are greatly reduced. In addition, due to the presence of chlorine atoms on the benzene ring, it not only reduces the electropositiveness on the benzene ring, but also may affect its Michael addition reaction with other thiol substances. Therefore, the antibacterial performance of N-ChPMI is lower than that of N-PMI.

Because N-PMI has partial electropositiveness and hydrophobicity, it is easy to interact with bacteria. In addition, membrane proteins are randomly distributed in the phospholipid area on the surface of the

bacterial cell membrane, which contains many cysteine residues and sulfhydryl groups. Perhaps it is due to the Michael addition reaction between N-PMI and membrane protein, as shown in Fig. 3, which changes the conformation of the membrane protein and affects the function of the membrane protein. It then causes the cells to shrink, the contents of the cells leak, and eventually the bacteria die.

3.3 Fluorescence Experiments

Fluorescence experiments can verify the interaction of N-PMI with bacterial cell membrane proteins[38]. There are three amino acid residues in the protein composition that can emit fluorescence, which are Phe, Tyr and Trp residues, and the emission wavelengths are 282nm, 303nm and 348nm, respectively. And their excitation wavelength is almost the same (296nm), only Phe has a lower excitation wavelength (258nm). Because the frequencies are relatively close, there will be energy transfer between Tyr and Trp residues, and even fluorescence quenching. The closer the spatial distance between these two residues, the easier the energy transfer between them.

Therefore, the fluorescence quenching agent KI was used to determine the amino acid residues, and the fluorescence spectra of the bacteria at the excitation wavelengths of 258nm or 296nm were measured after treatment with different concentrations of KI. The results were shown in Fig. 4[38]. It could be discerned that the fluorescence intensity of *E. coli* and *S. aureus* at the excitation wavelength of 296nm would slightly decrease with the increase of KI concentration. It indicated that Tyr and Trp residues mainly located inside or cranny of membrane. Thus, it could not reflect whether N-PMI would interact with the membrane protein. On the contrary, the fluorescence intensity at the excitation wavelength of 258nm decreased significantly with the increase of the concentration of KI. Therefore, it could be concluded that Phe were partly located on the surface of the bacteria cell membrane, which could sensitively reflect the interaction of N-PMI and membrane proteins.

Phe was selected as the target residue, and under the excitation wavelength of 258nm, the fluorescence quenching effect of the bacterial suspension with the change of N-PMI concentration was measured, and the result was shown in Fig. 5. It can be seen that as the concentration of N-PMI increases, the fluorescence intensity of Phe residues in *E. coli* and *S. aureus* continues to decrease, indicating that N-PMI does have a significant effect on bacterial membrane proteins. In addition, the fluorescence spectrum of Phe residues has also undergone a red shift, which means that the conformation of the membrane protein may have changed.

According to the fluorescence quenching mechanism, the fluorescence quenching phenomenon can be divided into static quenching and dynamic quenching, and it follows the Stern-Volmer equation[36].

$$\frac{F_0}{F} = 1 + K_q \tau_0 [Q] = 1 + K_{SV}[Q]$$

Where, F_0 and F are fluorescence intensities without and with the fluorescence quenching agent respectively, and K_q is dynamic fluorescence quenching rate constant of biomolecule. τ denotes the

lifetime of the fluorescence source in biological macromolecules (about 10 ~ 8 s), while [Q] denotes the concentration of the quenching agent[39, 40].

The mechanism of fluorescence quenching tells that dynamic quenching is a process in which the quencher interacts with the excited fluorescent molecule and does not affect the structure and physiological activity of the membrane protein. The rate constant of dynamic quenching is generally less than 2×10^{10}. Static quenching is a process in which the quencher and fluorescent molecules (membrane protein) form a type of complex or intermolecular complex, resulting in a decrease in fluorescence intensity[35, 41]. In general, the quenching rate constant of static quenching is significantly higher than the maximum dynamic quenching rate constant K_q (2×10^{10}) of the quencher for biological macromolecules.

Based on this mechanism, taking the concentration of N-PMI as the abscissa and the fluorescence intensity at the maximum emission peak as the ordinate, the fluorescence quenching curves of Phe residues in *E. coli* and *S. aureus* were shown in Fig. 5. It can be seen that N-PMI has obvious fluorescence quenching effect and is concentration-dependent. In addition, the Stern-Volmer curve showing the relationship between F_0/F and [Q] is also tried in Fig. 6. According to the calculation of the slope of the fitted straight line, the dynamic quenching rate constants K_q were 9.87×10^{11} and 7.85×10^{11} (for *E. coli* and *S. aureus*), respectively, which were significantly higher than 2×10^{10}. This indicates that the process of fluorescence quenching of membrane protein caused by N-PMI belongs to static quenching, which affects the conformation and physiological activity of membrane protein.

In contrast, the results in Fig. 7 show that N-PSI has almost no effect on the fluorescence intensity of *E. coli* and *S. aureus* membrane proteins, indicating that the interaction between N-PSI and bacterial cells is weak. It can also be confirmed that the antibacterial effect of N-PMI is mainly dependent on the interaction of its five-membered ring carbon-carbon double bond with membrane proteins.

3.4 Fluorescent visualization of permeation of membrane

FITC, as a low molecular mass (389 Da) green fluorescent probe, cannot pass through the cytoplasmic membrane of intact cells and emit fluorescence by interacting with non-specific enzymes in the cell. Only after N-PMI could interact with the cytoplasmic membrane and destroy it, FITC can interact with non-specific enzymes in the cell to emit fluorescence. Therefore, in the control sample that is not in contact with N-PMI in Fig. 8(a)–(b), although live *E. coli* can be seen in the photograph of the phase contrast microscope (PCM) in Fig. 8a, there doesn't appear any fluorescence also in the photograph of the laser confocal fluorescence microscope (LCM) in Fig. 8b. Although the fluorescence cannot be seen also in the PCM photo of the sample incubated with N-PMI for 60 minutes (Fig. 8c), the fluorescence emitted is clearly seen in the LCM photo of the sample incubated with N-PMI in Fig. 8d. It shows that the cell plasma membrane must have been destroyed by N-PMI. Figure 8e shows that the sample clearly exhibits fluorescence in the focused scan photos of the x-y plane, y-z plane and x-z plane. This indicates that bacterial membrane protein is the primary target of N-PMI, and then changes the conformation of the

membrane protein, which ultimately leads to the rupture of the membrane and the death of the bacteria[42].

3.5 Observation of cell morphology change

The field emission scanning electron microscope was used to observe the cell morphology and membrane changes as shown in Fig. 9. In the control group (Fig. 9a, b), a complete typical rod-shaped structure was observed in untreated *E. coli* cells, and the membrane surface was smooth and bright. In contrast, after N-PMI treatment, the cell morphology changed significantly, with different degrees of wrinkles, bumps, and even rupture (Fig. 9c, d). From the intuitive microscopic appearance, it directly shows that the morphological changes and rupture of cell membranes can be caused by N-PMI.

3.6 The leakage of K^+, Ca^{2+} and Mg^{2+} from the cell after treatment with N-PMI

Regulating the cation balance is of great significance to the survival and growth of bacteria. Among them, K^+, Ca^{2+} and Mg^{2+} are the keys to balance the cell plasma membrane charge, and therefore help maintain the intracellular pH value and membrane potential[43, 44]. ICP-OES was used to detect the extracellular metal ion concentration of the eluate before and after N-PMI treatment, and the results are shown in Fig. 10. The concentration of K^+, Ca^{2+} and Mg^{2+} in the eluate after N-PMI treatment is higher than that of the untreated bacteria eluate, indicating that N-PMI depolarizes the membrane, breaks the cation balance, and destroys various biochemical functions in the cell. Eventually cause the bacteria to die. In addition, as the contact time between bacteria and N-PMI increases, the loss of K^+ and Ca^{2+} tends to increase. Compared with K^+, Ca^{2+}, the loss of Mg^{2+} gradually tends to maintain at the level of 0.28mg/L.

3.7 Preparation and Antibacterial property of MMA-co-PMI copolymers and acrylic coatings

Based on the above discussion of the antibacterial mechanism of N-PMI, and our laboratory's previous research on reactive extrusion, it is worth exploring what kind of functional copolymer will be produced by copolymerizing N-PMI into the PMMA molecular chain. Although some PMMA human implants have been proven to be suitable for human use, bacterial infections and implant failure have caused scientists and surgeons to pay much attention to their antibacterial modification. Therefore, based on the previous research[31, 45], taking full advantage of the self-accelerating effect, the radical bulk copolymerization of MMA and wt.5% N-PMI in a twin-screw extruder was achieved through reactive extrusion polymerization, successfully obtaining a higher molecular weight and distribution narrow PMMA-co-5%PMI copolymer. Estimated from the ratio of copolymer to raw material, the single-pass conversion rate was 84%, and unpolymerized MMA (bp.100–101℃) was released under reduced pressure. According to the ratio of MMA/N-PMI raw materials, it can be calculated that approximately no more than 0.8wt% of N-PMI remains in the copolymer due to its higher boiling point (bp.162–163°C). The content of N-PMI in the

copolymer, molecular weight and its distribution are shown in Table 2, and its mechanical and heat resistant properties are shown in Table 3.

Table 2 Macromolecular weight and its distribution of PMMA-co-N-PMI

Samples	$M_n \times 10^{-4}$	$M_w \times 10^{-4}$	MWD
MMA-co-5%PMI	6.82	10.64	1.56
Commercial PMMA	4.31	6.94	1.61

Table 3 Mechanical and heat resistant properties of PMMA-co-N-PMI

Samples	T_g (°C)	Tensile strength (MPa)	Impact strength (KJ/m^2)	Flexural strength (MPa)
MMA-co-5%PMI	128.15	77.2 ± 2.0	22.3 ± 0.4	120.5 ± 2.6
Commercial PMMA	113.59	75.0 ± 1.8	20.4 ± 0.7	118.7 ± 3.0

It can be clearly seen from Table 2 that the molecular weight and distribution of PMMA-co-PMI copolymer is very similar to that of commercially available PMMA, which means that it can be used for injection molding to prepare various products. It can also be clearly seen from Table 3 that the flexural strength of the PMMA-co-PMI copolymer are superior to those of the usual commercially available PMMA. Especially in terms of heat resistance, its glass transition temperature (T_g) is almost 15°C higher than that of the latter, which provides favorable conditions for the PMMA-co-PMI copolymer to withstand boiling water sterilization. In addition, the composition of the copolymer is the same as the raw material ratio and the T_g is significantly increased. It clearly shows that the monomer N-PMI has randomly entered the segment of the PMMA molecular chain, not as predicted by the classic reactivity ratio[31]. The appearance and transparency of the PMMA-co-PMI copolymer sheet (2mm thick) with an N-PMI content of 5% is compared with that of commercially available PMMA as shown in Figure 10. It can be seen that the transparency is only slightly lower than that of pure PMMA. These are enough to show that PMMA-co-PMI is a random copolymer, and it is better to replace pure PMMA. However, since the PMMA-co-PMI copolymer uses the N-PMI monomer that can interact with the cell membrane of bacteria and rupture the cell membrane, which will eventually lead to the death of the bacteria. Can it play the same role while being copolymerized into the copolymer?

Therefore, the MMA-co-PMI copolymer was pulverized, and the antibacterial properties before and after washing were measured. In addition, the copolymer is hot-pressed into a thin sheet and tested by the zone of inhibition method to determine whether there was an antibacterial component oozing out of the sample.

Three vinyl monomers of MMA, GMA and BA are copolymerized in ethyl acetate solvent to form acrylic coatings with a T_g of 66°C and a molecular weight of 5.6×10^4. Then 0.5% and 1% of N-PMI was added into it, respectively, and after being uniformly mixed, the mixture was poured on the glass plate to form a film, and then it was dried in stages to form a film. It was crushed, and the antibacterial performance before and after washing was tested by the shaking method. The results were also listed in Table 4. It can be seen that the good solubility of N-PMI in organic solvents makes it evenly distributed in the acrylic paint, and the paint film has a good antibacterial effect. In addition, the leaching performance of the acrylic coating was tested by the bacteriostatic zone test, and the results are also shown in Fig. 11. It can be clearly seen that the acrylate coating layer containing 0.5% and 1% N-PMI also showed tiny bacteriostasis circles with similar dimensions as the PMMA-co-5%PMI sample. This clearly shows that N-PMI has very good compatibility with the matrix resin no matter in the PMMA-co-N-PMI system or in the PMMA-co-PBA-co-PGMA system, so that the free N-PMI is difficult to ooze out of the matrix resin system. This makes the PMMA-co-N-PMI system and the PMMA-co-PBA-co-PGMA coating system mixed with N-PMI have extremely good antibacterial effects, while only having a small inhibition zone and long-lasting antibacterial function.

The above research clearly shows that the antibacterial performance of any resin matrix containing N-PMI is related to the exudation of free N-PMI in the mixed system. In the PMMA-co-N-PMI system, although the comonomer contained 5% of the total mass of N-PMI, the N-PMI that participated in the copolymerization no longer had the antibacterial function. This can be verified from the Table 4. Because the antibacterial rate of PMMA-co-5% N-PMI system is not as good as PMMA-co-PBA-co-PGMA system mixed with 1% N-PMI, especially after washing. If the antibacterial function is still available after copolymerization of N-PMI, then the antibacterial performance should not decrease after washing, because it is impossible to lose the N-PMI after the copolymerization, but the fact is the opposite. In fact, the aforementioned antibacterial mechanism of N-PMI had clearly shown that the antibacterial function of N-PMI was caused by the interaction of its double bond with the sulfur group in the bacterial phospholipid layer, resulting in the rupture of the cell plasma membrane. Therefore, if the double bond is lost, the antibacterial function is lost.

Table 4 Antimicrobial Rates of MMA-co-N-PMI polymers and acrylic coatings

Samples	Antimicrobial rates against *E. coli* (%)			Antimicrobial rates against *S. aureus* (%)		
	Before washing	Cycles of water washing		Before washing	Cycles of water washing	
		5	10		5	10
PMMA	0	0	0	0	0	0
MMA-co-5%PMI	99	99	98	99	99	98
COATING	0	0	0	0	0	0
COATING-0.5%N-PMI	98	98	98	99	99	99
COATING-1%N-PMI	99	99	99	99	99	99

4 Conclusion

N-PMI is a multifunctional monomer with excellent antimicrobial function. Its antibacterial mechanism is that the double bond in its molecule can interact with the sulfur group in the bacterial membrane protein, changing its conformation and rupturing the cell plasma membrane. The contents leak and eventually cause the death of the microorganism. Therefore, once the double bond participates in the polymerization, N-PMI loses its antibacterial function. N-PMI can achieve azeotropic copolymerization with MMA through reactive extrusion polymerization, and does not follow the law of reactivity ratio of classic copolymerization. N-PMI with a content of 5% can be evenly inserted into the PMMA chain segment during the copolymerization reaction, thereby increasing the T_g of pure PMMA by up to 15°C, which provides the PMMA-co-PMI copolymer with resistance to boiling water sterilization advantageous conditions. In addition, the copolymer is superior to the commercially available pure PMMA in terms of bending strength and modulus. At the same time, N-PMI with a content of 5% has little effect on the transparency of PMMA after participating in the copolymerization. Moreover, the trace amount of residual N-PMI makes the material have excellent antibacterial function, and the bacteriostatic zone is extremely small, which provides an excellent guarantee for the safety and durability of the material. As a medical biological material, the PMMA-co-PMI copolymer has a good industrialization application prospects.

Declarations

Acknowledgments

The authors are grateful for the financial support from the National Natural Science Foundation of China (No.50573020).

Compliance with ethical standards

Conflict of interest The authors declare that they have no conflict of interest.

References

1. G.J. Gabriel, A. Som, A.E. Madkour, T. Eren, G.N. Tew, Infectious disease: Connecting innate immunity to biocidal polymers. Materials Science & Engineering R **57**(1–6), 28–64 (2007)
2. M.A. Pfaller, D.J. Diekema, Epidemiology of Invasive Candidiasis: a Persistent Public Health Problem. Clin. Microbiol. Rev. **20**(1), 133–163 (2007)
3. Nosocomial Bloodstream Infections in United States Hospitals, A Three-Year Analysis. Clinical Infectious Diseases (2):239–244
4. A. Shorr, V. Gupta, X. Sun, R. Johannes, J. Spalding, Y. Tabak, Burden of early-onset candidemia: Analysis of culture-positive bloodstream infections from a large US database. Critical care medicine **37**, 2519–2526 (2009). doi:10.1097/CCM.0b013e3181a0f95d quiz 2535.
5. K.K. Kumarasamy, M.A. Toleman, T.R. Walsh, J. Bagaria, F. Butt, R. Balakrishnan, U. Chaudhary, M. Doumith, C.G. Giske, S. Irfan (2010) K.K. Kumarasamy, M.A. Toleman, T.R. Walsh et al. Emergence of a new antibiotic resistance mechanism in India, Pakistan, and the UK: a molecular, biological, and epidemiological study. Lancet Infect Dis. 2010;10(9):597–602. Lancet Infectious Diseases 10:597–602
6. A.J. Hunt, V.L. Budarin, S.W. Breeden, A.S. Matharu, J.H. Clark, Expanding the potential for waste polyvinyl-alcohol. Green Chem. **11**(9), 1332–1336 (2009)
7. Z. Li, C. Jie, C. Wei, D. Wei, G. Yong, Permanent antimicrobial cotton fabrics obtained by surface treatment with modified guanidine. Carbohyd. Polym. **180**, 192 (2018)
8. L. Lou, Y. Koike, Y. Okamoto, A novel copolymer of methyl methacrylate with N-pentafluorophenyl maleimide: High glass transition temperature and highly transparent polymer. Polymer **52**(16), 3560–3564 (2011). doi:10.1016/j.polymer.2011.05.032
9. L. Lou, A. Tagaya, Y. Ide, Y. Koike, Y. Okamoto, Copolymers of methyl methacrylate with N-trifluorophenyl maleimides: High glass transition temperature and low birefringence polymers. J. Polym. Sci., Part A: Polym. Chem. **50**(17), 3530–3536 (2012). doi:10.1002/pola.26137
10. G.R. Shan, Z.X. Weng, Z.M. Huang, Z.R. Pan, Studies on the microstructure of vinyl/N-phenylmaleimide copolymers by NMR and their applications. J. Appl. Polym. Sci. **77**(12), 2581–2587 (2015)
11. A. Omayu, A. Matsumoto, Thermal Properties of N-Phenylmaleimide-Isobutene Alternating Copolymers Containing Polar Groups to Form Intermolecular and Intramolecular Hydrogen Bonding. Polym. J. **40**(8), 736–742 (2008). doi:10.1295/polymj.PJ2008073
12. Y. Igarashi, K. Yagami, R. Imai, S. Watanabe, Antimicrobial activities of some N -alkylmaleimides. J. Ind. Microbiol. **6**(3), 223–225 (1990)
13. M. Sortino, P. Delgado, S. Juárez, J. Quiroga, R. Abonía, B. Insuasty, M. Nogueras, L. Rodero, F.M. Garibotto, R.D. Enriz, S.A. Zacchino, Synthesis and antifungal activity of (Z)-5-arylidenerhodanines. Bioorg. Med. Chem. **15**(1), 484–494 (2007). doi:https://doi.org/10.1016/j.bmc.2006.09.038

14. M. Sortino, F. Garibotto, V. Cechinel Filho, M. Gupta, R. Enriz, S. Zacchino, Antifungal, cytotoxic and SAR studies of a series of N-alkyl, N-aryl and N-alkylphenyl-1,4-pyrrolediones and related compounds. Bioorg. Med. Chem. **19**(9), 2823–2834 (2011). doi:https://doi.org/10.1016/j.bmc.2011.03.038
15. M. Sortino, V. Cechinel Filho, R. Corrêa, S. Zacchino, N-Phenyl and N-phenylalkyl-maleimides acting against Candida spp.: Time-to-kill, stability, interaction with maleamic acids. Bioorg. Med. Chem. **16**(1), 560–568 (2008). doi:10.1016/j.bmc.2007.08.030
16. K. Takatori, T. Hasegawa, S. Nakano, J. Kitamura, N. Kato, Antifungal Activities of N-Substituted Maleimide Derivatives. Microbiol. Immunol. **29**, 1237–1241 (1985). doi:10.1111/j.1348-0421.1985.tb00913.x
17. S.A. Zacchino, E. Al, In vitro Antifungal Properties, Structure—Activity Relationships and Studies on the Mode of Action of N-Phenyl, N-Aryl, N-Phenylalkyl Maleimides and Related Compounds. ChemInform **36**, (26) (2005)
18. F.D. Suvire, M. Sortino, V.V. Kouznetsov, M.L.Y. Vargas, S.A. Zacchino, U.M. Cruz, R.D. Enriz, Structure–activity relationship study of homoallylamines and related derivatives acting as antifungal agents. Bioorg. Med. Chem. **14**(6), 1851–1862 (2006). doi:https://doi.org/10.1016/j.bmc.2005.10.036
19. Ippolito, Antonini, and, Rosaria, Volpini, and, DID. Ben, and (2008) Design, synthesis, and biological evaluation of new mitonafide derivatives as potential antitumor drugs - ScienceDirect. Bioorganic & Medicinal Chemistry 16 (18):8440–8446
20. A. Wu, Y. Xu, X. Qian, W. Jin, J. Liu, Novel naphthalimide derivatives as potential apoptosis-inducing agents: Design, synthesis and biological evaluation. Eur. J. Med. Chem. **44**(11), 4674–4680 (2009)
21. J.A. Yunes, A.A. Cardoso, R.A. Yunes, R. Corrêa, F.D. Campos-Buzzi, V.C. Filho, Antiproliferative effects of a series of cyclic imides on primary endothelial cells and a leukemia cell line. Zeitschrift Fur Naturforschung C A Journal of Biosciences **63**, (9–10) (2008)
22. S.M. Sondhi, R. Rani, P. Roy, S.K. Agrawal, A.K. Saxena (2009) ChemInform Abstract: Microwave-Assisted Synthesis of N-Substituted Cyclic Imides and Their Evaluation for Anticancer and Antiinflammatory Activities. ChemInform 40
23. V. Cechinel Filho, T. Pinheiro, R. Nunes, R. Yunes, A. Cruz, E. Moretto (1994) Antibacterial activity of N-phenylmaleimides, N-phenylsuccinimides and related compounds. Structure-activity relationships. Farmaco (Società chimica italiana: 1989) 49:675–677
24. N. Salewska, J. Boros-Majewska, I. Lacka, K. Chylinska, M. Sabisz, S. Milewski, M.J. Milewska, Chemical reactivity and antimicrobial activity of N-substituted maleimides. J. Enzyme Inhib. Med. Chem. **27**(1), 117–124 (2012). doi:10.3109/14756366.2011.580455
25. K.E. Machado, K.N. de Oliveira, H.M.S. Andreossi, LdS. Bubniak, A.C.R. de Moraes, P.C. Gaspar, EdS. Andrade, R.J. Nunes, M.C. Santos-Silva, Apoptotic Events Induced by Maleimides on Human Acute Leukemia Cell Lines. Chem. Res. Toxicol. **26**(12), 1904–1916 (2013). doi:10.1021/tx400284r
26. A. Carmona-Ribeiro, L. de Melo Carrasco, Cationic Antimicrobial Polymers and Their Assemblies. Int. J. Mol. Sci. **14**(5), 9906–9946 (2013)

27. M.A.R. Raycroft, K.E. Racine, C.N. Rowley, J.W. Keillor, Mechanisms of Alkyl and Aryl Thiol Addition to N-Methylmaleimide. J. Org. Chem. **83**(19), 11674–11685 (2018). doi:10.1021/acs.joc.8b01638
28. K.Y. Koltunov, G.K.S. Prakash, G. Rasul, G.A. Olah (2006) Superacidic Activation of Maleimide and Phthalimide and Their Reactions with Cyclohexane and Arenes. European Journal of Organic Chemistry 2006 (21):4861–4866. doi:https://doi.org/10.1002/ejoc.200600486
29. A. Souffrin, C. Croix, M.-C. Viaud-Massuard (2012) Efficient and General Protocol for Sonogashira Cross-Coupling Reactions of Maleimides. European Journal of Organic Chemistry 2012 (13):2499–2502. doi:https://doi.org/10.1002/ejoc.201101811
30. S. Varun, Kumar, Rangan, Mitra, A. Bhattarai, Vipin, Nair (2011) Reaction on Water: A Greener Approach for the Thia Michael Addition onN-Aryl Maleimides. Synthetic Communications
31. P. Zhan, J. Chen, A. Zheng, T. Huang, H. Shi, D. Wei, X. Xu, Y. Guan (2019) Preparation of methyl methacrylate-maleic anhydride copolymers via reactive extrusion by regulating the trommsdorff effect. Materials Research Express 6 (2). doi:10.1088/2053-1591/aaf13c
32. X. Yuan, Y. Guan, S. Li, A. Zheng, Anionic bulk polymerization to synthesize styrene–isoprene diblock and multiblock copolymers by reactive extrusion. Journal of Applied Polymer ence **131**(2), - (2014)
33. X. Yuan, J. Wang, D. Shan, A. Zheng, Styrene/isoprene/butadiene integrated rubber prepared by anionic bulk polymerization in a twin-screw extruder. Polym. Eng. Sci. **55**(5), 1163–1169 (2015)
34. X. Ding, F. Chen, Y. Guan, A. Zheng, D. Wei, X. Xu, Preparation and properties of an antimicrobial acrylic coating modified with guanidinium oligomer. J. Coat. Technol. Res. **17**(6), 1505–1513 (2020). doi:10.1007/s11998-020-00370-z
35. X. Ye, X. Li, L. Yuan, B. Zhang, Interaction between houttuyfonate homologues and erythrocyte plasma membrane of rabbit in vitro. Colloids & Surfaces A Physicochemical & Engineering Aspects **279**(1–3), 218–224 (2006)
36. E.L. Gelamo, C.H. Silva, H. Imasato, M. Tabak, Interaction of bovine (BSA) and human (HSA) serum albumins with ionic surfactants: spectroscopy and modelling. Biochim. Biophys. Acta **1594**(1), 84–99 (2002). doi:10.1016/s0167-4838(01)00287-4
37. A. Sharma, S. Srivastava, Anti- Candida activity of two-peptide bacteriocins, plantaricins (Pln E/F and J/K) and their mode of action. Fungal Biology **118**(2), 264–275 (2014)
38. X.F. Liu, Y.M. Xia, F. Yun, Effect of metal ions on the interaction between bovine serum albumin and berberine chloride extracted from a traditional Chinese Herb coptis chinensis franch - ScienceDirect. J. Inorg. Biochem. **99**(7), 1449–1457 (2005)
39. J.R. Lakowicz, *Quenching of Fluorescence* (Principles of Fluorescence Spectroscopy, 1999)
40. J.R. Lakowicz, G. Weber, Quenching of fluorescence by oxygen. A probe for structural fluctuations in macromolecules. Biochemistry **12**(21), 4161–4170 (1973)
41. E.L. Gelamo, M. Tabak, Spectroscopic studies on the interaction of bovine (BSA) and human (HSA) serum albumins with ionic surfactants. Spectrochim Acta A Mol Biomol Spectrosc **56A**(11), 2255–2271 (2000). doi:10.1016/s1386-1425(00)00313-9

42. L. Ying, W. Chang, Z. Ming, X. Li, H. Lou, Diorcinol D Exerts Fungicidal Action against Candida albicans through Cytoplasm Membrane Destruction and ROS Accumulation. PLoS ONE **10**(6), e0128693 (2015)
43. Z. Jaromír, S. Hana (2012) Plasma-membrane hyperpolarization diminishes the cation efflux via Nha1 antiporter and Ena ATPase under potassium-limiting conditions. FEMS Yeast Research (4):4
44. S. Cyert, Martha (2013) Regulation of Cation Balance in Saccharomyces cerevisiae. Genetics
45. P. Zhan, J. Chen, A. Zheng, H. Shi, T. Wu, D. Wei, X. Xu, Y. Guan (2020) Methyl methacrylate-styrene copolymers prepared by utilizing the Trommsdorff effect in an inverted two-stage extruder. Materials Research Express 7 (9). doi:10.1088/2053-1591/abb4fd

Figures

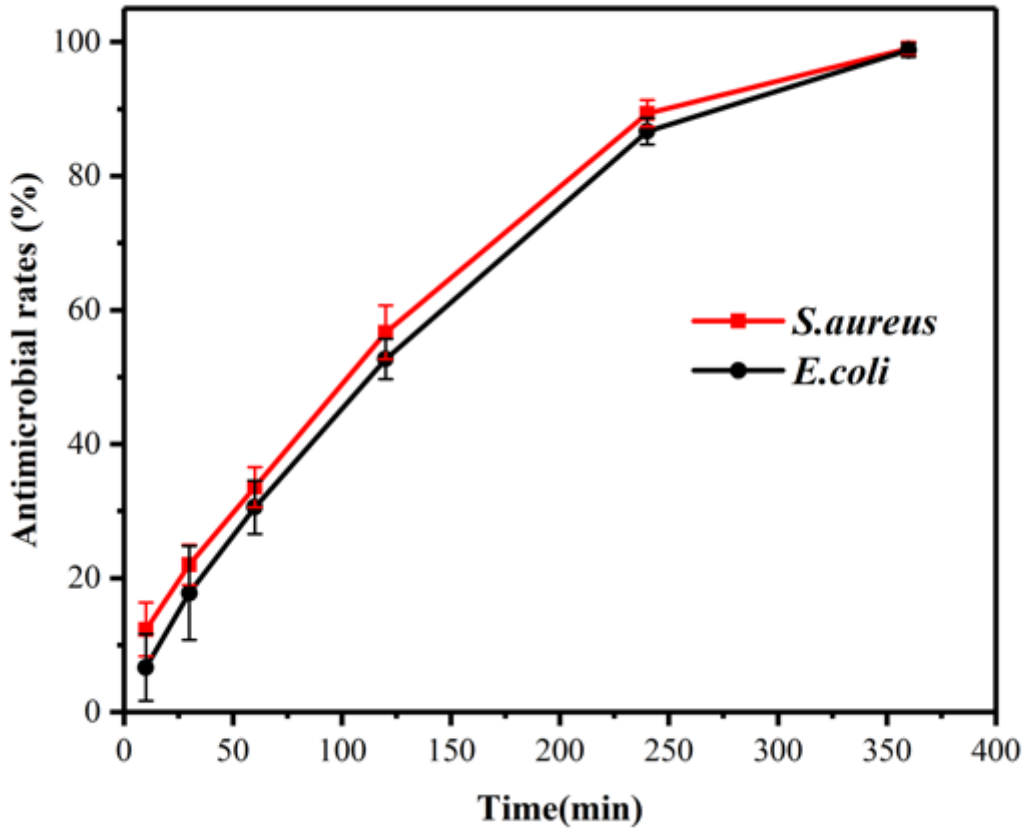

Figure 1

Antibacterial rate-contact time curves of N-PMI against E.coli and S. aureus

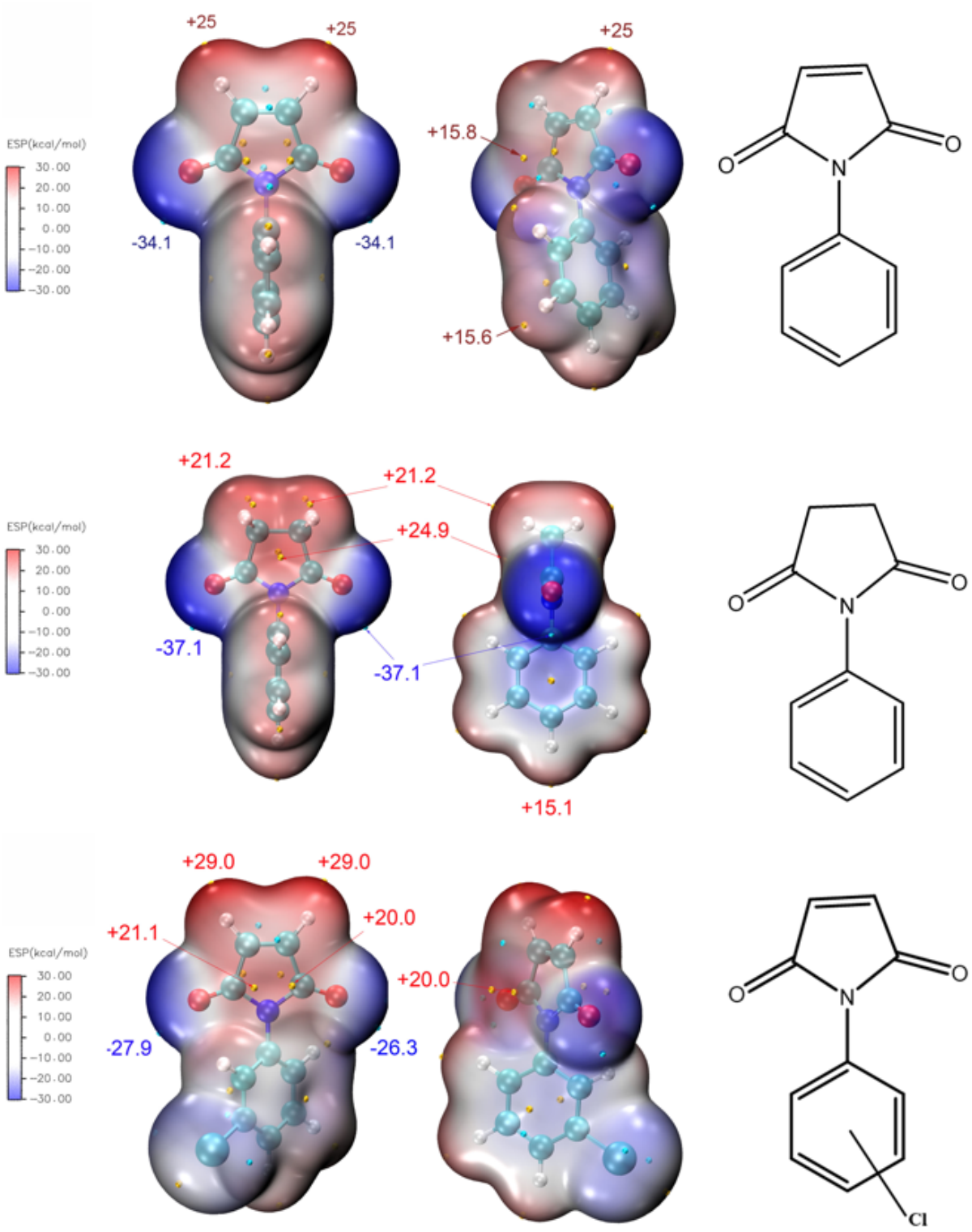

Figure 2

Molecular electrostatic potential (ESP) maps on the 0.001 au isosurface of (a) N-PMI, (b) N-PSI, and (c) N-ChPMI. (Energy values are given in kcal/mol).

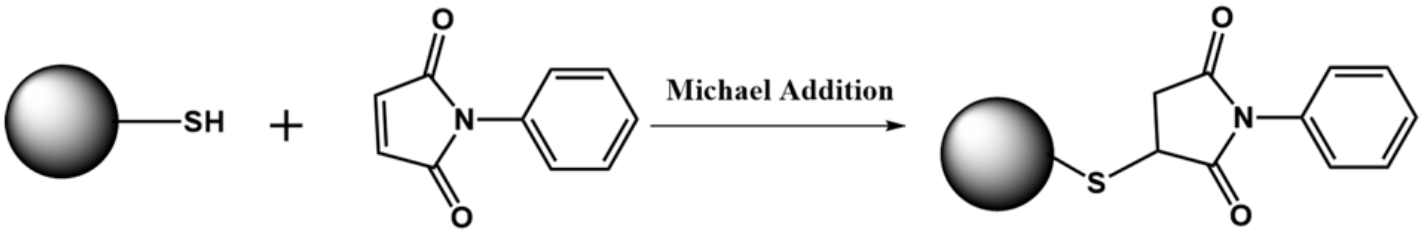

Figure 3

Scheme of reaction between N-PMI and cysteinyl residues in membrane protein

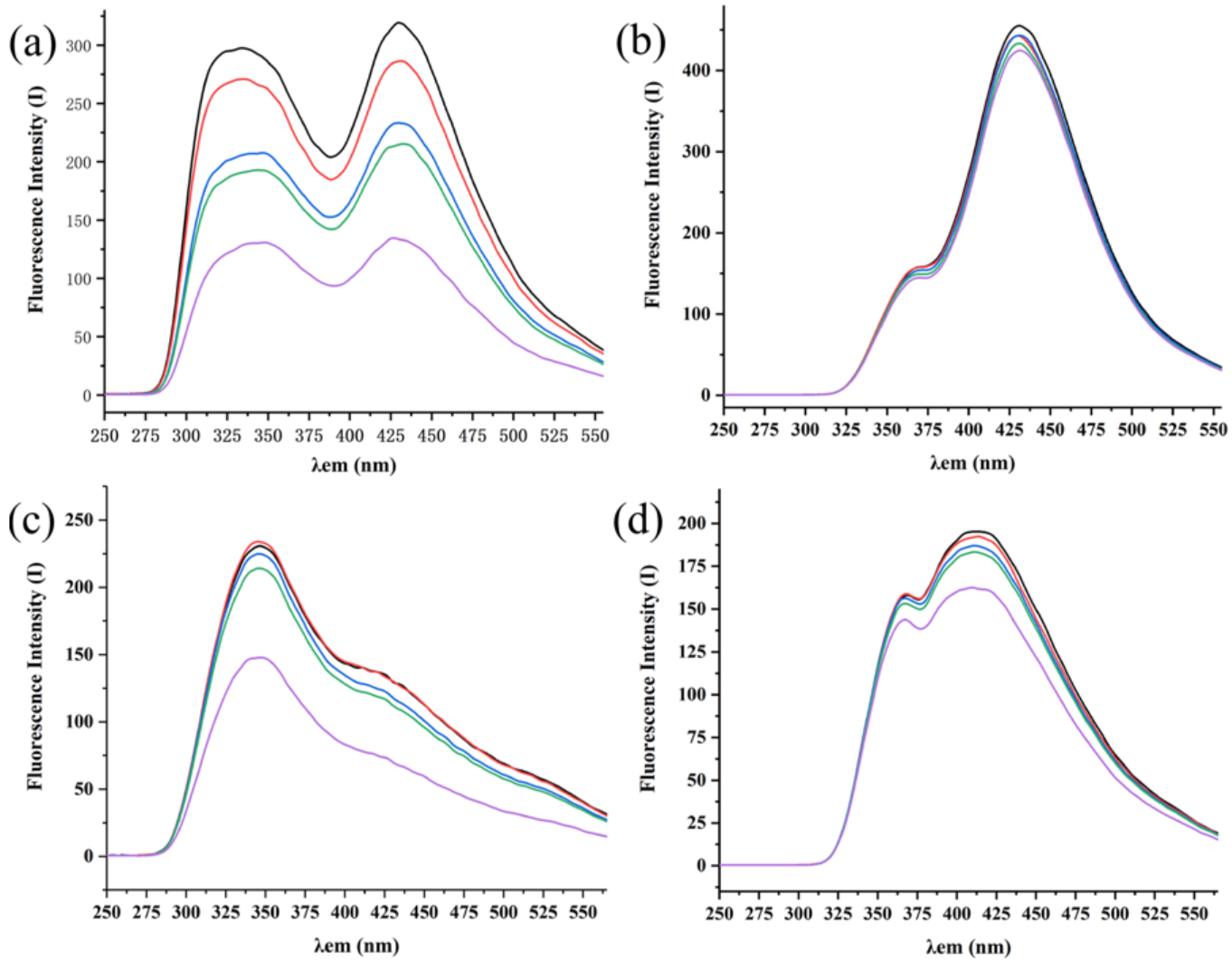

Figure 4

The influence of the concentration of N-PMI on the fluorescence intensity in the emission wavelength range of 200-600 nm at the excitation wavelengths of 258 nm of (a) E. coli membrane protein and (c) S. aureus membrane protein, and at the excitation wavelengths of 297 nm of (b) E. coli membrane protein

and (d) S. aureus membrane protein, respectively Concentration of KI (from the top down) was: 0, 0.0125, 0.025, 0.05 and 0.1 mol/L, respectively.

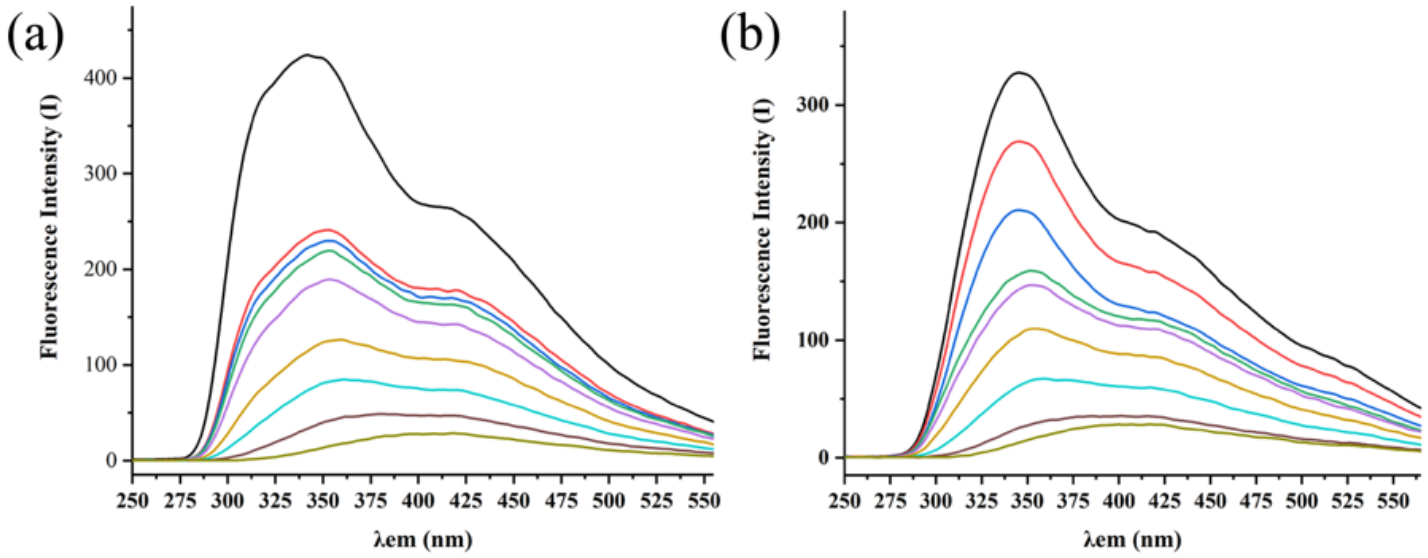

Figure 5

The influence of the concentration of N-PMI on the fluorescence intensity in the emission wavelength range of 200-600 nm at the excitation wavelengths of 258 nm of (a) E. coli membrane protein and (b) S. aureus membrane protein, respectively Concentration of N-PMI (from the top down) was: 0, 3.125, 6.25, 12.5, 25, 50, 100, 200 and 400 μg/mL, respectively

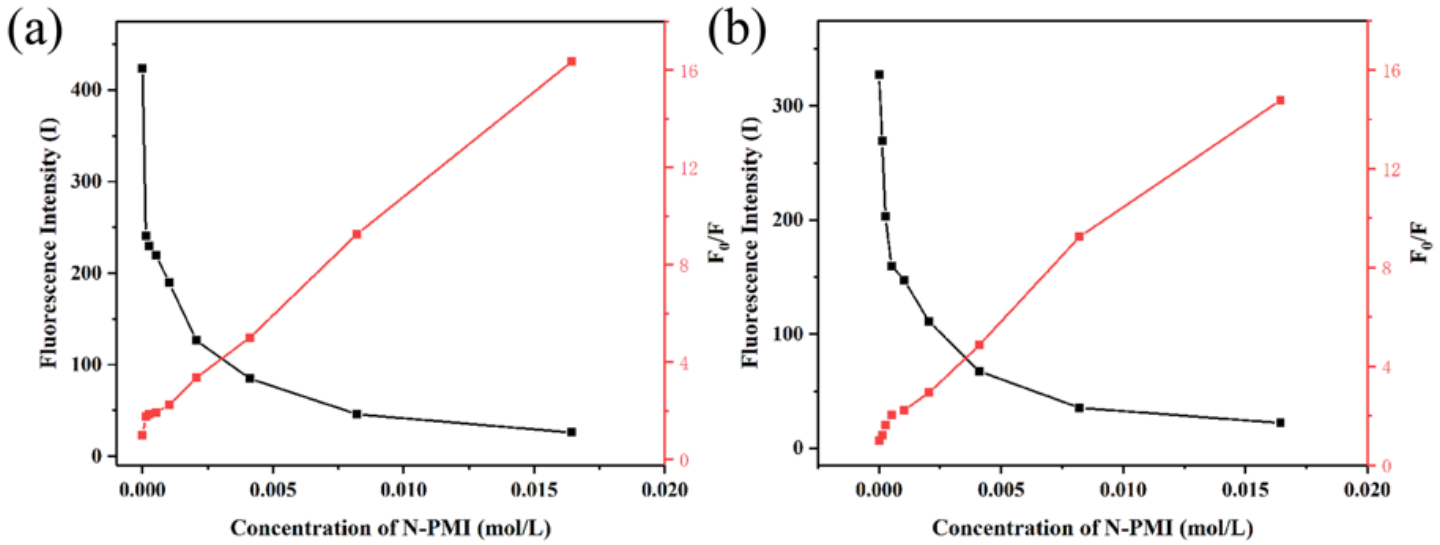

Figure 6

When the excitation wavelength is 258 nm, the effect of N-PMI on the fluorescence intensity of bacterial membrane protein at the maximum emission wavelength of 338 nm (black) and the corresponding Stern-Volmer curve (red). (a) E. coli; (b) S. aureus

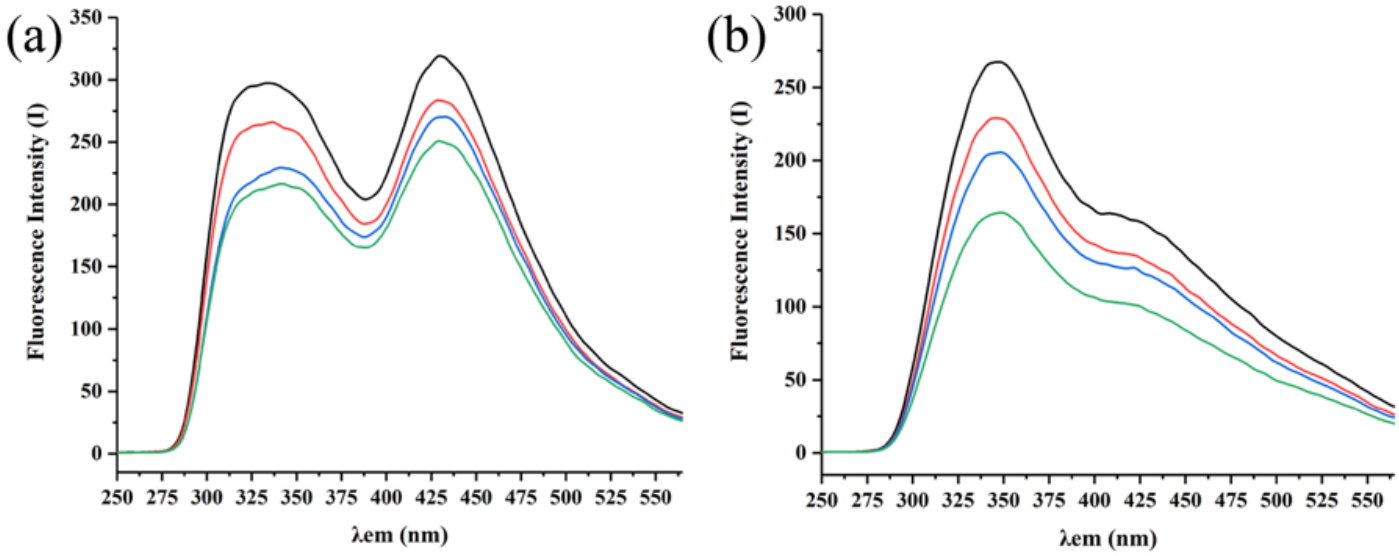

Figure 7

The influence of different concentrations of N-PSI on (a) E. coli and (b) S. aureus membrane protein fluorescence intensity in the 200-600 nm wavelength range when the excitation wavelength is 258 nm. Concentration of N-PSI (from the top down) was 0, 0.2, 0.4 and 0.8 mg/mL, respectively;

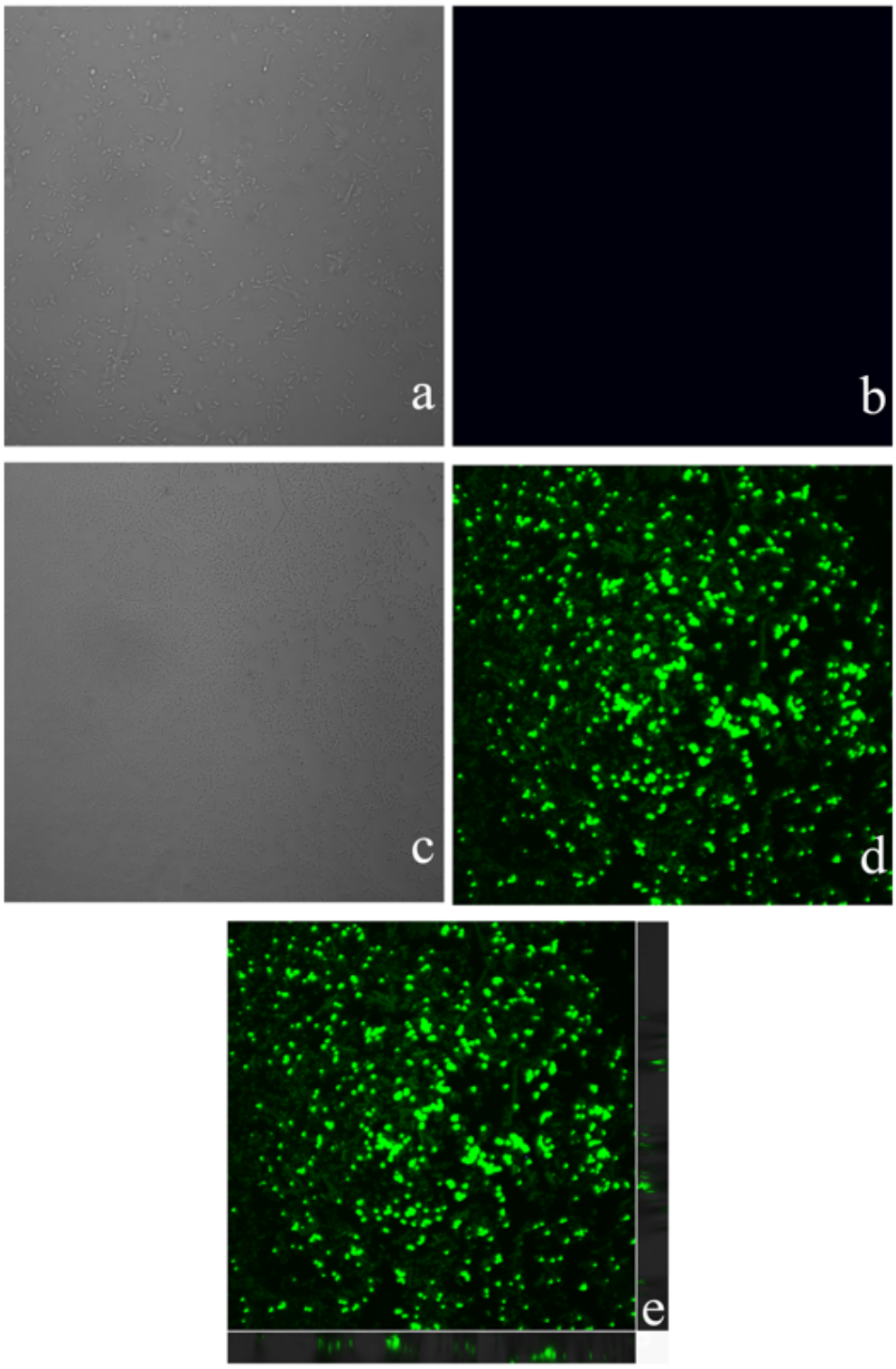

Figure 8

Laser confocal microscope (LCM) photos of 2×108 CFU/mL E. coli after FITC staining and co-incubation for 60 min with 40 mg/L N-PMI: (a) Phase contrast microscope (PCM) photo of control cells; (b) LCM photo of control cells; (C) PCM photo of the measured cells; (d) LCM photo of the measured cells; (e) LCM photos of xy (upper left), yz (upper right), xz (lower left) of the measured cells.

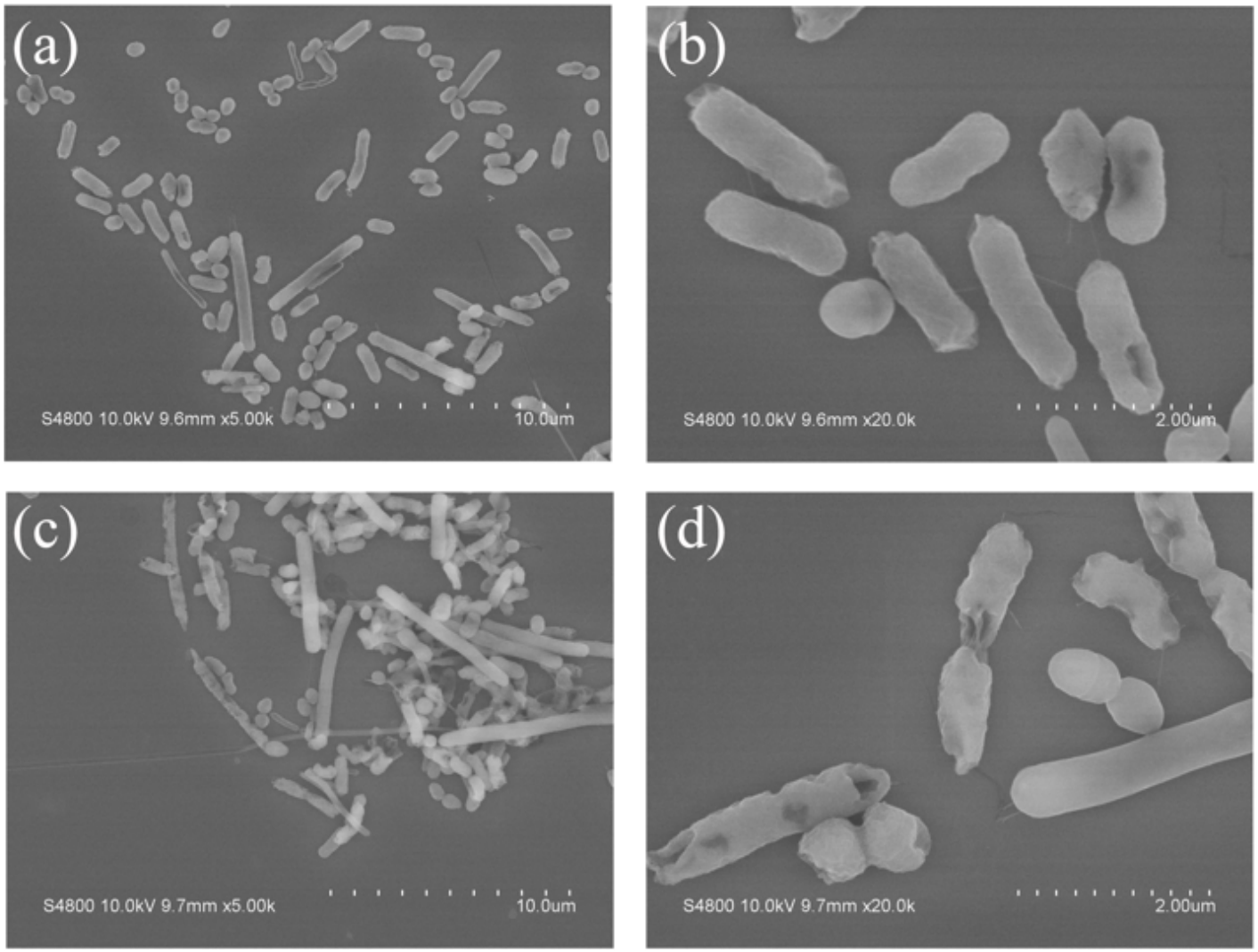

Figure 9

Observation of cell morphology change and membrane damage by field emission scanning electron microscope. Control bacteria (a, b); the 2× 108 CFU/mL E. coli was treated with 40 mg/L N-PMI for 60 min (c, d).

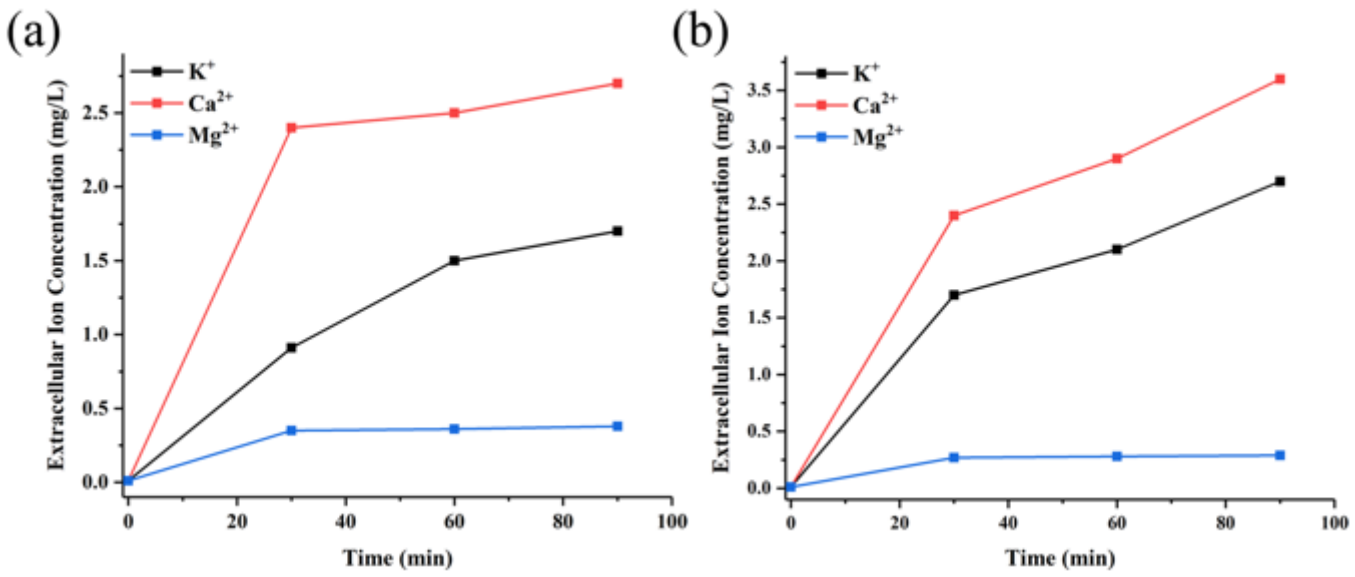

Figure 10

K+, Ca2+ and Mg2+ were lost from the cell when the bacteria were treated with 40 mg/L N-PMI at 28°C for 1 min, 30 min, 60 min and 90 min, (a) E. coli; (b) S. aureus The data was the mean ± standard deviation of 3 independent experiments

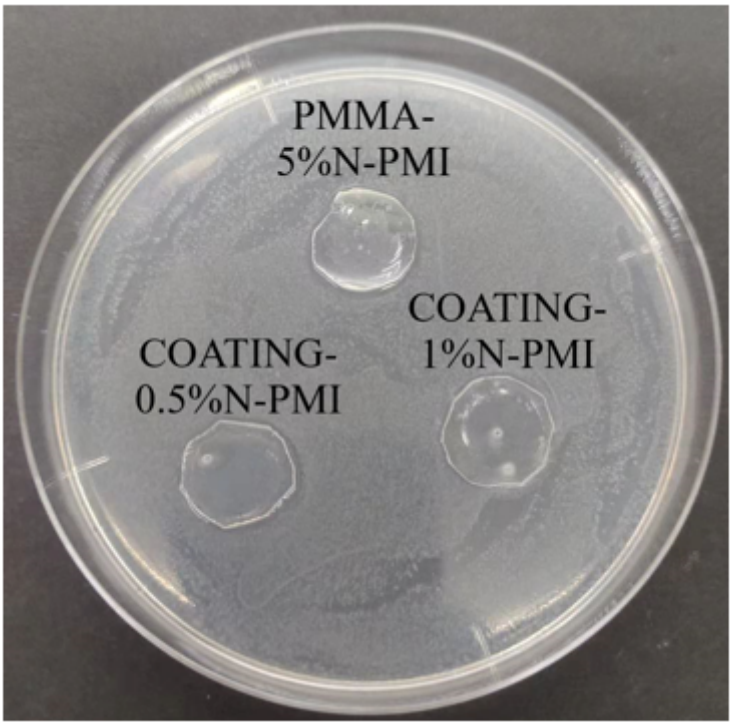

Figure 11

Photos of inhibition zone against E. coli of samples including MMA-co-5%PMI, COATING-0.5%N-PMI and COATING-1%N-PMI.

Supplementary Files

This is a list of supplementary files associated with this preprint. Click to download.

- GraphicalAbstract.png